*horticulturae*

MDPI

*Article*

# Insights into the *PYR/PYL/RCAR* Gene Family in Pomegranates (*Punica granatum* L.): A Genome-Wide Study on Identification, Evolution, and Expression Analysis

**Ke Yin [1,2], Fan Cheng [1,2], Hongfang Ren [1,2], Jingyi Huang [1,2], Xueqing Zhao [1,2] and Zhaohe Yuan [1,2,*]**

[1] Co-Innovation Center for Sustainable Forestry in Southern China, Nanjing Forestry University, Nanjing 210037, China; keyin@njfu.edu.cn (K.Y.); chengfan990427@njfu.edu.cn (F.C.); fangfang@njfu.edu.cn (H.R.); nanlinhjy@njfu.edu.cn (J.H.); zhaoxq402@njfu.edu.cn (X.Z.)
[2] College of Forestry, Nanjing Forestry University, Nanjing 210037, China
* Correspondence: zhyuan88@hotmail.com

**Abstract:** The response of plants to abiotic stress is intricately mediated by *PYR/PYL/RCARs*, key components within the ABA signal transduction pathway. Despite the widespread identification of *PYL* genes across diverse plant species, the evolutionary history and structural characteristics of these genes within the pomegranate (*Punica granatum* L.) remained unexplored. In this study, we uncovered, for the first time, 12 *PgPYLs* from the whole genome dataset of 'Tunisia', mapping them onto five chromosomes and categorizing them into three distinct subgroups (Group I, Group II, and Group III) through phylogenetic analysis. Detailed examination of the composition of these genes revealed similar conserved motifs and exon–intron structures among genes within the same subgroup. Fragment duplication emerged as the primary mechanism driving the amplification of the *PYL* gene family, as evidenced by intra-species collinearity analysis. Furthermore, inter-species collinearity analysis provided insights into potential evolutionary relationships among the identified *PgPYL* genes. Cis-acting element analysis revealed a rich repertoire of stress and hormone response elements within the promoter region of *PgPYLs*, emphasizing their putative roles in diverse signaling pathways. Upon treatment with 100 µmol/L ABA, we investigated the expression patterns of the *PgPYL* gene family, and the qRT-PCR data indicated a significant up-regulation in the majority of *PYL* genes. This suggested an active involvement of *PgPYL* genes in the plant's response to exogenous ABA. Among them, *PgPYL1* was chosen as a candidate gene to explore the function of the gene family, and the CDS sequence of *PgPYL1* was cloned from pomegranate leaves with a full length of 657 bp, encoding 218 amino acids. Tobacco transient expression analysis demonstrated a consistent trend in the expression levels of pBI121-*PgPYL1* and the related genes of the ABA signaling pathway, both of which increased initially before declining. This study not only contributes to the elucidation of the genomic and structural attributes of *PgPYL* genes but also provides a foundation for understanding their potential functions in stress responses. The identified conserved motifs, evolutionary relationships, and expression patterns under ABA treatment pave the way for further research into the *PgPYL* gene family's role in pomegranate biology, offering valuable insights for future studies on genetic improvement and stress resilience in pomegranate cultivation.

**Keywords:** pomegranate; *PYL* gene family; bioinformatics; gene expression



**Citation:** Yin, K.; Cheng, F.; Ren, H.; Huang, J.; Zhao, X.; Yuan, Z. Insights into the *PYR/PYL/RCAR* Gene Family in Pomegranates (*Punica granatum* L.): A Genome-Wide Study on Identification, Evolution, and Expression Analysis. *Horticulturae* **2024**, *10*, 502. https://doi.org/10.3390/horticulturae10050502

Academic Editor: Adriana F. Sestras

Received: 1 April 2024
Revised: 10 May 2024
Accepted: 11 May 2024
Published: 13 May 2024



## 1. Introduction

The pomegranate (*Punica granatum* L.), a member of the genus *Punica* within the family Lythraceae stands as a globally significant economic forest species [1]. Renowned for its nutrient-rich fruit, containing vitamins, proteins, minerals, tannins, and flavonoids, pomegranates enjoy increasing popularity among consumers [2]. Despite their cultivation in both northern and southern regions of China, pomegranates, like many fruit trees, grapple with various stresses ranging from high salinity, drought, and low temperatures

to nutritional deficiencies and pathogenic bacterial infestations during cultivation. These challenges substantially curtail their yield and quality, resulting in notable economic losses. Addressing this issue necessitates the identification of stress-resistant and high-quality genes in pomegranates, pursued through molecular methods and functional studies. The contemporary focus on excavating anti-stress genes in molecular breeding, facilitated by genome sequencing advancements, amplifies the significance of such investigations. The recent completion of pomegranate genome sequencing, including varieties like 'Taishanhong' [1], 'Dabenzi' [3], and 'Tunisia' [4], has furnished high-quality genomic maps, forming a critical knowledge foundation for comprehensive studies on pomegranate gene function, paving the way for systematic advancements in pomegranate molecular biology and genetic improvement.

Abscisic acid (ABA), a growth regulator of plants, orchestrates essential physiological functions, including embryo development, stomatal regulation, seed germination, and dormancy [5,6]. Notably, ABA assumes a central role in plants' responses to stress and adversity. When plants encounter abiotic stressors such as drought, hypersalinity, or low temperatures, a rapid increase in intracellular ABA content ensues. This surge regulates water balance and osmotic pressure, concurrently adjusting gene expression linked to adversity in response to environmental pressures [7]. The ABA signal transduction mechanism finely regulates ABA content in plants. This intricate pathway involves protein phosphatases 2C (*PP2C*) as negative regulators and sucrose nonfermenting 1-related protein kinases2 (*SnRK2*) as positive regulators [8–10]. In the absence of ABA, the *PYR/PYL/RCAR* receptors fail to interact with *PP2C*, allowing *PP2C* to exhibit high phosphatase activity. This, in turn, inhibits *SnRK2* kinase activity, impeding downstream gene expression in the ABA signal transduction pathway [11,12]. Conversely, under adverse conditions like hypersalinity, drought, or low temperatures, a rapid increase in ABA content prompts interaction with ABA receptors, initiating a cascade that inhibits *PP2C*, unleashing *SnRK2* kinase activity. Activated *SnRK2* phosphorylates downstream transcription factors, including *ABI5*, *AREB1*, and *AREB2*, which then attach to cis-acting elements in the downstream ABA-responsive genes' promoters, initiating the expression of ABA signaling-related genes [13–17].

The *PYR/PYL/RCAR* gene family, characterized by a conserved START structural domain [18], comprises fourteen members in *Arabidopsis*, divided into three subgroups, among which *AtPYL7*, *AtPYL8*, *AtPYL9*, and *AtPYL10* were classified under Group I, while *AtPYL4*, *AtPYL5*, *AtPYL6*, *AtPYL11*, *AtPYL12*, and *PgPYL13* were categorized under Group II, and *AtPYR1*, *AtPYL1*, *AtPYL2*, and *AtPYL3* were assigned to Group III [19]. Notably, overexpressing specific members, such as *AtPYL4*, *AtPYL5*, and *AtPYL9*, has demonstrated enhanced resistance to drought while simultaneously increasing sensitivity to ABA in *Arabidopsis* [12,20,21]. In tobacco, this gene family has been identified in 29 *NtPYLs* genes which played an important role in seed development, germination, and response to ABA, particularly in drought tolerance [22]. This gene family has been discovered in various plants, such as rice (13) [23], maize (13) [24], strawberry (11) [25], tomato (14) [26], and grape (6) [27], with evidence suggesting that the overexpression of ABA receptors heightens transgenic plants' ABA sensitivity and tolerance to abiotic stresses. For instance, in maize, *ZmPYL8*, *ZmPYL9*, and *ZmPYL12* play pivotal roles in drought tolerance [28]. The overexpression of *PtPYRL5* and *PtPYRL1* in poplar enhances reactive oxygen species scavenging [29], while *OsPYL/RCAR5* positively regulates ABA signal transduction, enhancing rice's resistance to drought and salinity stress and increasing seeds' sensitivity to ABA during seed germination and seedling growth stages [30,31].

Despite extensive exploration of the *PYL* gene family in various plants, its investigation in pomegranates (*Punica granatum* L.) has been limited. In alignment with the genomic information of the 'Tunisia' variety, we identified members of the *PYL* gene family in pomegranate and conducted a comprehensive analysis encompassing the chromosomal location, physicochemical properties of proteins, phylogenetic relationships, exon–intron gene structures, cis-acting elements, and collinearity. Additionally, we scrutinized the expression patterns of each member under ABA treatment. Finally, according to the results

of the evolutionary tree, the amino acid sequence homology of *PgPYL1* and *AtPYL4* proteins is high, suggesting that their gene function may be similar, whereas *AtPYL4* has previously been reported to exhibit increased drought resistance in *Arabidopsis*. Therefore, the *PgPYL1* gene was cloned and analyzed for transient expression in tobacco. This study lays a foundational groundwork for further research into the functional aspects of the *PgPYL* gene family, offering prospective candidate genes for genetic engineering and pomegranate breeding.

## 2. Materials and Methods

### *2.1. Experimental Plant Materials and Treatment*

The focus of the study was the 'Tunisia' variety of pomegranates. Hard branches that were one year old were chosen and clipped to a height of 10 to 15 cm. Subsequently, the cuttings were placed in pots measuring 32 cm by 25 cm and covered with a 1:1 mixture of perlite and charcoal soil for potting. The cuttings were cultivated under a 16 h light and 8 h dark photoperiod in a controlled environment chamber at Nanjing Forestry University. The diurnal temperature was sustained at 25 °C/18 °C, with 70% relative humidity. After 65 days of incubation, pomegranate cuttings exhibiting uniform, robust, and disease-free growth were chosen as the experimental materials for ABA treatment. Pomegranate cuttings were treated with 100 µmol/L ABA. The solution was evenly sprayed on the pomegranate leaves, and the spraying was stopped when water droplets were about to drop from the leaf edge. Three biological replications were required for the treatment, and 15 pomegranate cuttings were used as one biological replication. Pomegranate leaves were randomly collected at 0 (control check), 2, 6, 12, 24, and 48 h after treatment; quick-frozen in liquid nitrogen; and then brought back to the laboratory and stored in an ultra-low-temperature refrigerator at −80 °C for subsequent experiments.

### *2.2. Genome-Wide Identification of PgPYL gene Family*

We downloaded the pomegranate whole genome information ('Tunisia' ASM765513v2) and the *PYL* sequences of *Arabidopsis* from the online program NCBI (http://www.ncbi.nlm.nih.gov/, accessed on 5 September 2023) and TAIR (http://www.Arabidopsis.org/, accessed on 5 September 2023), respectively. To identify the *PYL* gene family members in pomegranates, we employed two different methods. Firstly, the *PYL* sequences of *Arabidopsis* were used to find *PgPYLs* in the pomegranate genome with BLAST [32] software. The E-value was set to default ($E < e^{-10}$). Second, the Pfam (http://pfam-legacy.xfam.org/, accessed on 6 September 2023) was used to acquire the Hidden Markov Model (HMM) that represented the distinctive domain Polyketide_cyc2 (PF10604) of the *PYL* gene family proteins. The sequences of pomegranate were subsequently screened using the HMMER [33] software. Furthermore, the results obtained by the above two methods were pooled to acquire the candidate gene ID, and the protein sequence of the candidate gene was extracted by Tbtools software. Finally, we used the website SMART (http://smart.embl.de/, accessed on 6 September 2023) for candidate gene screening and revalidation of conserved structural domains and manually removed redundant sequences without Polyketide_cyc2 domains. Twelve confirmed members were finally obtained in pomegranate sequences. Based on the gene registration numbers, they were named *PgPYL1~PgPYL12*. Subsequently, the chromosomal coordinate result of the acquired 12 genes was submitted to the MG2C [34] (http://mg2c.iask.in/mg2cv2.1/, accessed on 7 September 2023) for visualization.

### *2.3. Proteins Physicochemical Properties, Structural Analysis, and Subcellular Localization Prediction*

The fundamental physicochemical properties of the *PgPYL* gene family were recognized with Expasy-ProtParam [35] (http://web.expasy.org/protparam/, accessed on 7 September 2023). The prediction of signal peptides was conducted utilizing SignalP4.1 [36] (https://services.healthtech.dtu.dk/services/SignalP-4.1/, accessed on 7 September 2023). SoPMA [37] (http://npsa-pbil.ibcp.fr/cgi-bin/npsa_automat.pl?page=npsa_sopma.html,

accessed on 7 September 2023) was applied to analyze the secondary structure of *PgPYL* proteins, and Plant-mPloc [38] (http://www.csbio.sjtu.edu.cn/bioinf/plant-multi/, accessed on 7 September 2023) was accessed to predict subcellular localization.

### 2.4. Phylogenetic Analysis

The *PYL* amino acid sequences in pomegranate were compared with those in *Arabidopsis*, grape, tomato, and strawberry plants with the Clustal W alignment tool. MEGA 11.0 [39] was employed to frame an evolutionary tree with the maximum likelihood (ML) method (Bootstrap = 1000). Subsequently, the files containing the evolutionary tree data were uploaded to the iTOL online platform (https://itol.embl.de/, accessed on 8 September 2023) for visualization enhancement.

### 2.5. Conserved Domains, Conserved Motif, and Exon–Intron Structure Analysis

We used bioinformatics software DNAMAN 9.0 to compare the 12 acquired *PgPYL* sequences. The structural domains of the *PgPYL* proteins were predicted with Batch-CD-Search (https://www.ncbi.nlm.nih.gov/Structure/bwrpsb/bwrpsb.cgi/, accessed on 9 September 2023). We used the program MEME [40] (http://meme-suite.org/meme/tools/meme, accessed on 9 September 2023) to obtain a conserved motif analysis with motifs set to 12 and default parameters for other settings. In order to analyze the gene structure, the 12 *PgPYL* genes' annotation data were extracted from genome-wide gff files in pomegranates and submitted to the GSDS [41] (http://gsds.gao-lab.org/, accessed on 9 September 2023). Subsequently, the protein structural domains, conserved motifs, and gene structures of *PgPYLs* were visualized with TBtools [42].

### 2.6. Promoter Cis-Acting Elements Analysis

We used software TBtools to extract sequences located 2000 bp upstream of the pomegranate genome start codon. Subsequently, potential cis-acting elements were identified using PlantCARE [43] (http://bioinformatics.psb.ugent.be/webtools/plantcare/html/, accessed on 10 September 2023), and the outcomes were also visualized by the software TBtools.

### 2.7. Collinearity and Selection Pressure Analysis

The MCScanX [44] program was applied to obtain the results of intraspecific collinearity in pomegranates for gene duplication pattern analysis. Circo plot of intraspecific collinearity was performed with TBtools and gene family member locations and collinearity were marked. The whole genome sequences in pomegranates were analyzed for interspecific collinearity with *Arabidopsis* and tomato by the MCScanX program, and the results of interspecific collinearity were presented with TBtools. To analyze the selection pressure of pomegranate, the Ka (non-synonymous substitution rate) and Ks (synonymous substitution rate) between *PgPYL* genes were calculated by DnaSP 5.0 [45] program.

### 2.8. RNA Extraction and Gene Clone

Total RNA was extracted from pomegranate leaf samples with the SteadyPure Plant RNA Extraction Kit (Accurate, Changsha, China). Subsequently, RNA was transcribed into cDNA by using cDNA synthesis kit (HiScript III RT SuperMix for qPCR (+gDNA wiper), Vazyme, Nanjing, China). Primer design was conducted using Primer Premier 5.0 software (Table S1), and primers were synthesized by Nanjing Tsingke Biotech Company, Nanjing, China.

The PCR amplification system comprised 50 μL total volume, consisting of 25 μL of 2× Rapid Taq Master Mix (Vazyme, Nanjing), 20 μL of dd$H_2O$, 2 μL of DNA template, and 1.5 μL of forward and reverse primers. The PCR reaction program was as follows: 95 °C, 5 min; 95 °C, 15 s; 54 °C, 20 s; 72 °C, 30 s with a total of 33 cycles; and 72 °C, 5 min. After the PCR products were separated by 1% agarose gel electrophoresis, the target bands were cut, and the products were recovered by DNA gel extraction kit (Tsingke, Nanjing).

Moreover, the recovered product was ligated to the laboratory-preserved vector pBI121 (constitutive promoter CaMV35S) using Clon Express® II One Step Cloning Kit (Vazyme, Nanjing). The ligation product was put into a 2 mL centrifuge tube with *Escherichia coli* DH5α receptor cell (Tsingke, Nanjing, China) at a ratio of 1:100 and transformed by heat shock method. Then antibiotic-free LB liquid medium was added to the centrifuge tube and incubated at 37 °C, 220 rpm for 40 min. The cultured fluid was evenly spread on the LB solid medium containing Kana antibiotic (concentration 50 μg/mL) and incubated at 37 °C for 16 h. When a single colony appeared in the medium, it was picked out and identified by PCR, the same PCR reaction program as above, and if a positive band appeared, it was sent to Nanjing Tsingke Biotech Company for sequencing. Finally, the sequence results obtained were translated into amino acid sequences using the ExPaSy-Translate website (https://web.expasy.org/translate/, accessed on 20 September 2023) and compared with DNAMAN software.

### *2.9. Tobacco Transient Expression*

The correctly sequenced pBI121-*PgPYL1* plasmid was transferred into *Agrobacterium tumefaciens* GV3101 (Tsingke, Nanjing, China) by freeze–thaw method. The operation was as follows: the plasmid and GV3101 receptor cell were put into the centrifuge tube at a ratio of 1:50, which was put into an ice bath for 10 min, followed by liquid nitrogen for 5 min, then a 37 °C water bath for 5 min and ice bath for 10 min. In addition, used an oscillation rate of 220 r/min, the activated Agrobacterium was injected at a ratio of 1:100 into 50 mL of LB liquid medium and allowed to incubate for 16 h at 28 °C. The cultured bacterial solution was centrifuged at 4000 r/min for 10 min to collect the bacteria, which were resuspended in the prepared resuspension solution (10 mmol/L MES + 10 mmol/L $MgCl_2.6H_2O$ + 100 mmol/L AS, pH = 5.7). After standing for 3 h, they were injected into tobacco leaves, while wild-type (WT) tobacco was used as a control. The tobacco leaves were picked on days 1, 3, 5, and 7 and stored at −80 °C for subsequent gene expression studies.

### *2.10. Analysis of Quantitative Real-Time PCR (qRT-PCR)*

Expression patterns of PgPYLs in pomegranate and tobacco leaves were detected using qRT-PCR. The Primer Premier 5.0 was used to design the specific quantitative primers (Table S1). The internal reference gene selected PgActin and NtActin. In addition, the online website Primer-BLAST (https://www.ncbi.nlm.nih.gov/tools/primer-blast/index.cgi?LINK_LOC=BlastHome, accessed on 5 September 2023) was used to check the specificity of the primers. The melting curve of the primers was verified as unimodal before the experiment.

The quantitative real-time PCR reaction system comprised 20 μL total volume, consisting of 10 μL of 2X SYBR® Green Pro Taq HS Premix (Accurate, Nanjing, China), 8.2 μL of RNase-free water, 1 μL of cDNA template (the RNA viscosity was about 150 ng/μL), and 0.4 μL of forward and reverse primers. The experiment was completed with Applied Biosystems 7500. The qRT-PCR reaction protocol was as follows: 95 °C, 30 s; 40 cycles of 95 °C, 5 s; and 60 °C, 30 s; and we collected melting curves with the instrument's default program. For each treatment, three technical and biological replicates had to be conducted. The relative expressions of *PgPYL* genes were analyzed by $2^{-\Delta\Delta CT}$ method [46]. The results were analyzed and plotted with SPSS 26.0 and GraphPad Prism 9 software, respectively.

### *2.11. Data Analysis*

The data are shown as the mean ± SD of the three biological replicates. Duncan's test ($p < 0.05$) in SPSS 26.0 was selected to analyze the data differences' significance, and GraphPad Prism 9.0 was used for data visualization.

## 3. Results

### *3.1. Genome-Wide Identification and Chromosomal Location of PgPYLs*

Through homology matching and de-redundancy, 12 *PgPYL* genes were identified in pomegranates. They were named *PgPYL1~PgPYL12* based on their gene accession numbers. The chromosomal localization of the *PgPYLs* was examined (Figure 1). The outcomes showed that these genes were sporadically dispersed over five pomegranate chromosomes. Specifically, four *PgPYLs* (*PgPYL3*, *PgPYL6*, *PgPYL10*, and *PgPYL12*) were located on chromosome 1, three *PgPYLs* (*PgPYL8*, *PgPYL9*, and *PgPYL11*) were distributed on chromosome 4, two *PgPYLs* (*PgPYL4*, *PgPYL5* and *PgPYL1*, *PgPYL2*) were located on chromosome 2 and 8 separately, and only *PgPYL* (*PgPYL7*) was distributed on chromosome 3. Notably, chromosomes 5, 6, and 7 did not exhibit any distribution of *PgPYLs*.

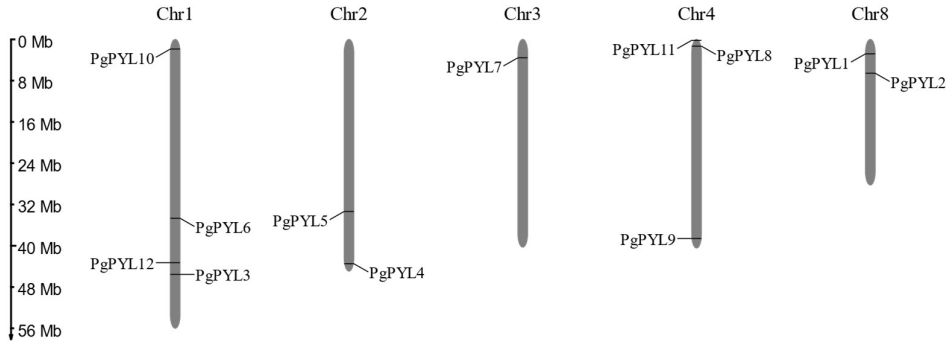


**Figure 1.** Chromosome distribution and localization of *PgPYL* genes.

### *3.2. Protein Physicochemical Properties, Structural Analysis, and Subcellular Localization Prediction of PgPYLs*

The results of the basic physical and chemical properties, as displayed in Table S2, show that the *PgPYL* proteins contained 135 (*PgPYL4*) to 248 (*PgPYL5*) amino acids, an average of 203. *PgPYL5* was the largest protein; in contrast, *PgPYL4* was the shortest protein, which showed significant variation from the other family members. The molecular weight (MW) varied from 14.78 kDa (*PgPYL4*) to 26.92 kDa (*PgPYL5*), with an average of 20.52 kDa. The theoretical isoelectric point (PI) ranged from 5.06 (*PgPYL2*) to 6.54 (*PgPYL1*), with an average of 6.02. These values fall within the acidic range, indicating that the *PgPYL* gene family consisted of acidic proteins. The instability index of the *PgPYL* proteins ranged from 30.61 (*PgPYL7*) to 53.99 (*PgPYL10*), with an average of 41.25. The instability index of *PgPYL2*, *PgPYL3*, *PgPYL7*, and *PgPYL8* is less than 40, indicating that they are stable proteins, while the stability index of the other eight *PgPYL* proteins is more than 40, indicating that they are unstable proteins. The aliphatic index ranged from 79.12 (*PgPYL8*) to 95.23 (*PgPYL1*), with a mean value of 88.44. The grand average of hydrophilicity ranged from −0.409 (*PgPYL11*) to −0.032 (*PgPYL1*), with an average of −0.257, which are negative, suggesting that *PgPYLs* are hydrophilic proteins. Moreover, none of the twelve *PgPYL* proteins had signal peptides according to the results of the signal peptide prediction, indicating that they are non-secretory proteins.

The SoPMA and Plant-mPloc were used to predict protein secondary structure and subcellular localization. As shown in Table S2, all *PgPYL* proteins consisted of four distinct forms of secondary structures, with α-helices, extended strands, and random coils dominating the secondary structures of all amino acid sequences. Regarding the structural elements, *PgPYL7* exhibited the most α-helices, while *PgPYL9* displayed the most β-turns. Additionally, *PgPYL10* demonstrated the highest number of random coils. Furthermore, among the *PgPYL* proteins, *PgPYL4* and *PgPYL10* had the highest numbers of extended strands in comparison to the other *PgPYL* proteins.

Subcellular localization prediction analyses revealed that *PgPYL1*, *PgPYL2*, *PgPYL5*, *PgPYL6*, *PgPYL7*, *PgPYL8*, and *PgPYL10* were localized in the cytoplasm. *PgPYL4* and *PgPYL9* were found to be localized in the chloroplasts and nucleus, while *PgPYL11* and

*PgPYL12* were specifically localized in the chloroplasts. In contrast, *PgPYL3* differed from the other members of the *PgPYL* gene family in that it was exclusively localized in the nucleus.

### *3.3. Phylogenetic Analysis of the PgPYL gene Family*

To investigate the phylogenetic and developmental connections among the *PgPYL* gene family members, we conducted an alignment of the *PYL* sequences from pomegranate, *Arabidopsis*, grape, tomato, and strawberry plants (Table S3). Subsequently, an evolutionary tree was built with the maximum likelihood method. The phylogenetic development outcome (Figure 2) revealed that the *PYL* gene family members were categorized into three subgroups (Group I, Group II, and Group III). According to the phylogenetic tree grouping, *PgPYL4*, *PgPYL9*, *PgPYL11*, and *PgPYL12* were classified under Group I; while *PgPYL1*, *PgPYL5*, *PgPYL6*, and *PgPYL10* were categorized under Group II; and *PgPYL2*, *PgPYL3*, *PgPYL7*, and *PgPYL8* were assigned to Group III. The phylogenetic tree indicated that all *PgPYLs* were dispersed among various subgroups, suggesting that they possess unique functions. It can be seen from the evolutionary tree that in Group I, the three *FvPYL* genes (*FvPYL7*, *FvPYL8*, and *FvPYL16*) and the five *FvPYL* genes (*FvPYL1*, *FvPYL3*, *FvPYL4*, *FvPYL13*, and *FvPYL14*) of strawberry plants each formed a more independent clustered evolutionary branch. In Group II, the three *SlPYL* genes (*SlPYL15*, *SlPYL17*, and *SlPYL18*) of tomatoes, the three *AtPYL* genes (*AtPYL11*, *AtPYL12*, and *AtPYL13*) of *Arabidopsis*, and the two *PgPYL* genes (*PgPYL3* and *PgPYL8*) of pomegranates in Group III showed the same phenomenon. Therefore, we speculate that different members of the same species may have experienced gene duplication events during evolution. In addition, through phylogenetic analysis, we could infer similar functions of the *PgPYL* gene from genes with high homology to those of pomegranates. For example, we found that the amino acid sequences of *PgPYL1*, *SlPYL9*, and *AtPYL4* have a high degree of identity percentage, and the genes *SlPYL9* and *AtPYL4* have also been reported to enhance drought resistance [21,47], so we hypothesize that *PgPYL1* may have similar functions.

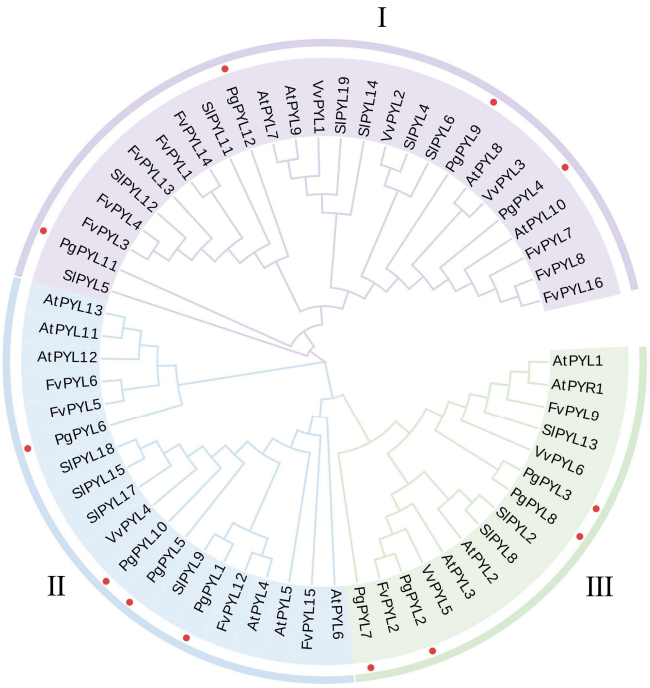


**Figure 2.** Phylogenetic analysis of *PYL* genes in pomegranate (*Punica granatum* L.), *Arabidopsis* (*Arabidopsis thaliana* L.), grape (*Vitis vinifera* L.), tomato (*Solanum lycopersicum* L.), and strawberry (*Fragaria vesca* L.). The different colors indicate different subgroups. The red dots represent *PgPYLs*.

### *3.4. Conserved Domains, Conserved Motif, and Intron–Exon Structure Analysis of PgPYLs*

The *PgPYL* gene family sequences were analyzed using bioinformatic software DNAMAN 9.0. The structural domain of the *PYL* proteins, which served as a direct receptor for ABA, was characterized by four highly conserved loops. Among them, the conserved structural domain CL2 was referred to as the gate or proline-cap. Similarly, the conserved structural domain CL4 was recognized as the latch or leucine-lucker. The GATE-LATCH structure of the *PYL* proteins changed their interaction with the ABA molecule, resulting in the formation of a surface that interacted with *PP2C* proteins while immobilizing the ABA molecule. Thus, the GATE-LATCH structure, which comprises two conserved structural domains, CL2 and CL4, is a distinctive characteristic of *PYL* proteins participating in the ABA signaling pathway, serving as receptors of ABA. The multiple amino acid sequence comparison of the *PgPYL* proteins (Figure 3) revealed that all 12 *PgPYL* proteins possess conserved structural domains, CL2 and CL4. Several amino acid sites within the structural domains were also observed to be conserved and invariant. Although some of the conserved structural domains of *PgPYL* genes exhibited base mutations, it was speculated that this phenomenon could be associated with their regulatory function. In the conserved CL2 structural domains of *PgPYL3* and *PgPYL6*, it was found that the serine(S) was substituted with threonine(T) in "SGLPA", which did not impact its function as a gatekeeper, as has been demonstrated in sorghum [48].

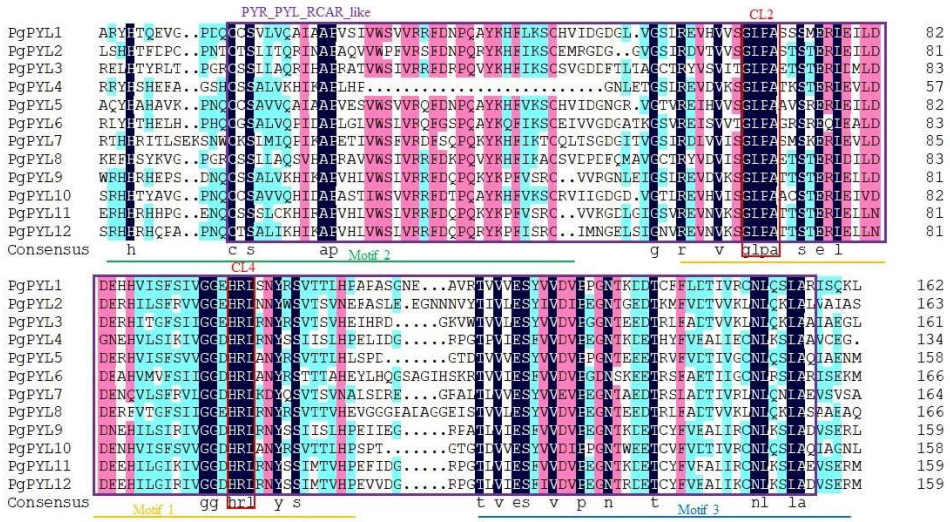


**Figure 3.** Multiple alignments of *PgPYL* proteins. The black, pink, and blue backgrounds indicate complete (100%), high (75%), and moderate (50%) conservatism, respectively. The purple square represents *PYR/PYL/RCAR* protein structural domains, and the red square represents conserved structural domains CL2 and CL4. The yellow, green, and blue lines represent motif1, motif2, and motif3, respectively.

The *PgPYL* proteins' conserved motifs were observed via the website MEME. Twelve conserved motifs are shown in Figure 4a, of which motif1, motif2, and motif3 have the most amino acids. The distribution of the conserved motifs in *PgPYLs* was established based on the motif analysis results (Figure 4b-B), and it was discovered that the number of motifs varied among the different *PgPYLs*, which confirmed the diversity of their functions. The *PgPYL* gene family encompasses 3–7 motifs, with *PgPYL7* exhibiting the fewest motifs, while *PgPYL9*, *PgPYL11*, and *PgPYL12* display the most motifs. All gene family members except *PgPYL4* contain motif1, motif2, and motif3. Therefore, it is presumed that motif1, motif2, and motif3 serve as the functional bases of *PgPYL* genes, and the positional regions of motif1, motif2, and motif3 also correspond to the positional regions of the conserved domains of PYR_PYL_RCAR_like protein. Except for *PgPYL7*, the majority of *PgPYLs* exhibit distinct motifs, indicating potential specificity in their biological functions. For example, *PgPYL3* and *PgPYL8* both contain motif4 and motif9, and *PgPYL6* features motif11.

Various arrangements and combinations of motifs constitute the specific structure of genes, and the allocation of these specific motifs serves as the theoretical foundation for gene categorization.

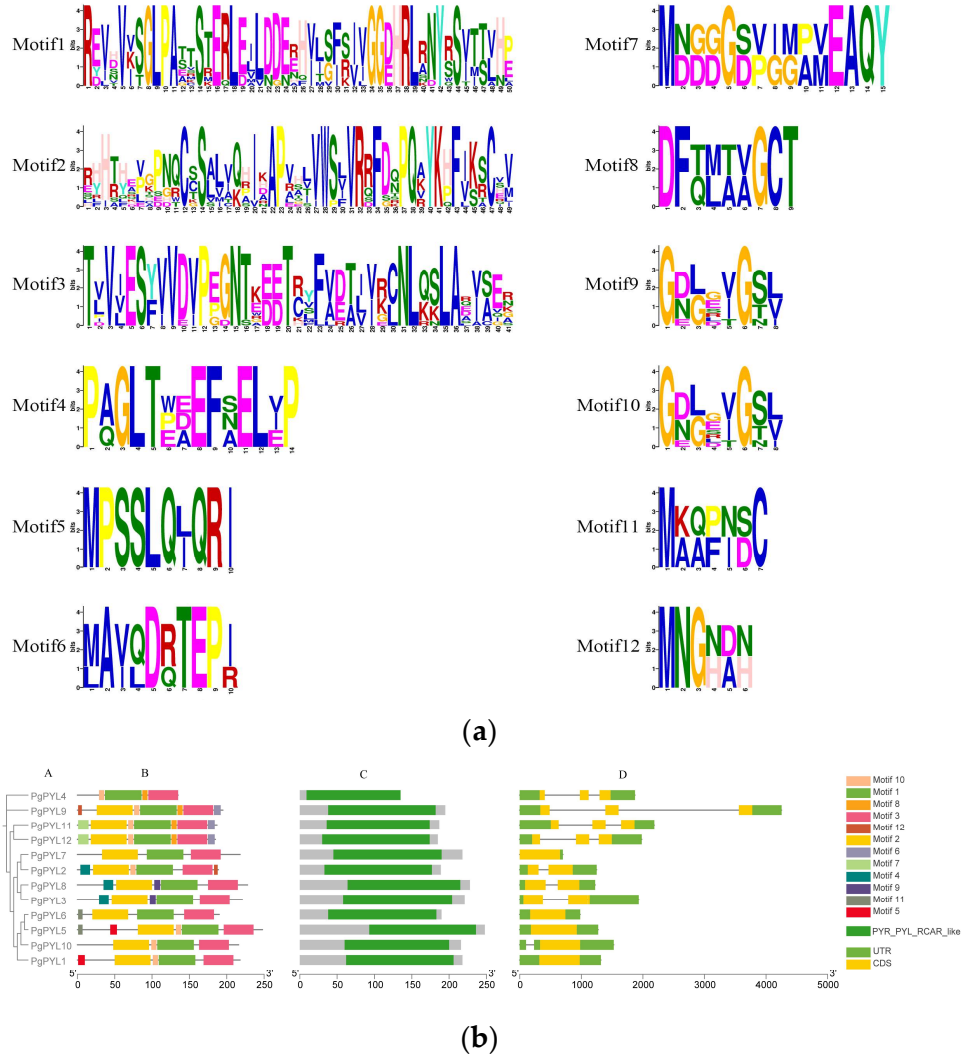


**Figure 4.** (**a**) Protein conserved motifs of the *PgPYL* genes. The horizontal coordinate indicates the position of the amino acid in the sequence, the vertical coordinate indicates the amino acid conservation, and the height of the amino acid letter indicates the frequency of occurrence; (**b**) conserved motifs and gene structure among *PgPYLs*. (A) The phylogenetic tree of *PgPYLs*; (B) conserved motifs of *PgPYLs*; (C) conserved domains of *PYR_PYL_RCAR* in *PgPYLs*; (D) exon–intron structure of *PgPYL* genes.

To explore the gene structure of the *PgPYL* gene family, the 12 *PgPYL* genes' structures were analyzed to attain deeper insights into the evolutionary process of the *PgPYL* gene family. The results are shown in Figure 4b-D; as far as gene structure is concerned, the *PgPYL* gene family does not fall into the category of exon-enriched gene families, which only contain 1–3 exons. It has been demonstrated that most genes exhibiting similar exon–intron structures within a specific gene family have akin evolutionary relationships. There are three distinct exon–intron structures in the *PgPYL* gene family. Specifically, four members of Group I (*PgPYL4*, *PgPYL9*, *PgPYL11*, and *PgPYL12*) possess three exons and two introns. Another member of Group II (*PgPYL10*) exhibits two exons and one intron, while the remaining three members of Group II (*PgPYL1*, *PgPYL5*, and *PgPYL6*) display one exon and no introns. Additionally, three members of Group III (*PgPYL2*, *PgPYL3*, and *PgPYL8*) have two exons and one intron, while the remaining member of Group III

(*PgPYL7*) has one exon and no introns. The observed outcome may be attributed to the insertion or removal of introns within the gene structure.

### *3.5. Cis-Acting Elements Analysis of PgPYLs*

We analyzed the cis-acting elements of 12 *PgPYLs* and visualized the results with TBtools to better comprehend the potential functions (Table S4). The results revealed that the promoter region contained 33 cis-acting elements (Figure 5), which divided into three classifications: stress-response, growth and developmental, and hormone-response. Certain *PgPYLs*' promoter regions exhibited MYB binding sites, which are important in drought induction (MBS) [49] and light response (MRE), respectively. Apart from the MRE, the promoter regions of *PgPYLs* contained G-box, Box 4, GATA-motif, and GT1-motif, which related to light response [50]. This observation suggests that *PgPYLs* may be regulated by light. Furthermore, the twelve *PgPYL* genes possessed low-temperature-response elements (LTR), and seven *PgPYL* genes contained wound-responsive elements (WUN-motif). We also identified several elements that are directly linked to the growth and development, including meristem expression regulatory elements (CAT-box), cell cycle regulation element (MSA-like), an element controlling circadian rhythms (circadian), and an element involved in zein metabolism regulation (O2-site). Furthermore, the *PgPYL* promoter region was found to contain five kinds of hormone-related components, including the abscisic acid response element, growth hormone response elements, methyl jasmonate response elements, gibberellin response elements, and salicylic acid response element. This finding indicates that other hormones also regulate the response of *PgPYL* to ABA and may entail a more intricate signal transduction network.

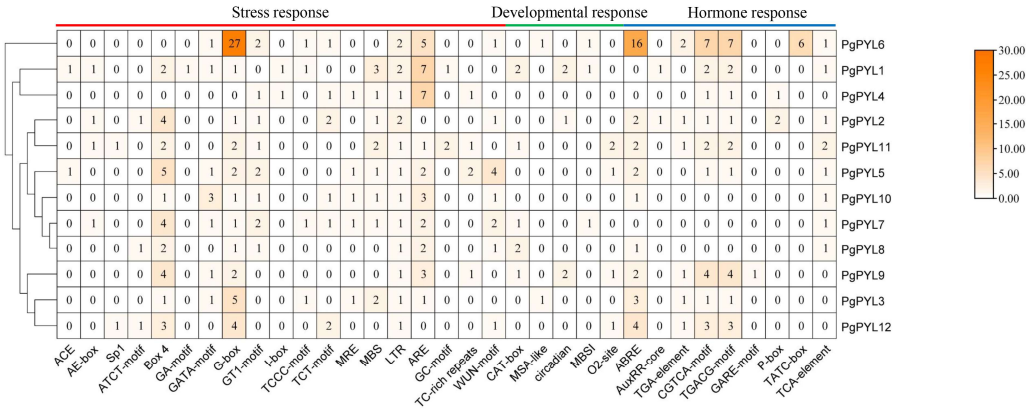


**Figure 5.** The cis-acting element analysis of *PgPYL* genes. The numbers represent the number of cis-acting elements. The red line represents stress response. The green line represents development response. The blue line represents hormone response.

### *3.6. Collinearity and Selection Pressure Analysis of PgPYLs*

The creation of new genes and functional differentiation depended on gene duplication [51]. Analysis of whole-genome duplication could provide a more comprehensive exploration of the evolutionary relationships in the *PgPYL* genes. In the *PgPYLs'* duplication events analysis, six pairs of genome duplications were identified (Figure 6): *PgPYL1* and *PgPYL5*, *PgPYL3* and *PgPYL8*, *PgPYL4* and *PgPYL9*, *PgPYL4* and *PgPYL12*, *PgPYL9* and *PgPYL11*, and *PgPYL9* and *PgPYL12*. The outcome implies that gene duplication might have produced certain *PgPYL* genes and potentially facilitated the extended evolution of *PgPYL* gene family. In addition, we found that *PgPYL2*, *PgPYL6*, *PgPYL7* and *PgPYL10* appear to have no other genes with which they are collinear, suggesting that these genes may have evolved without replication events.

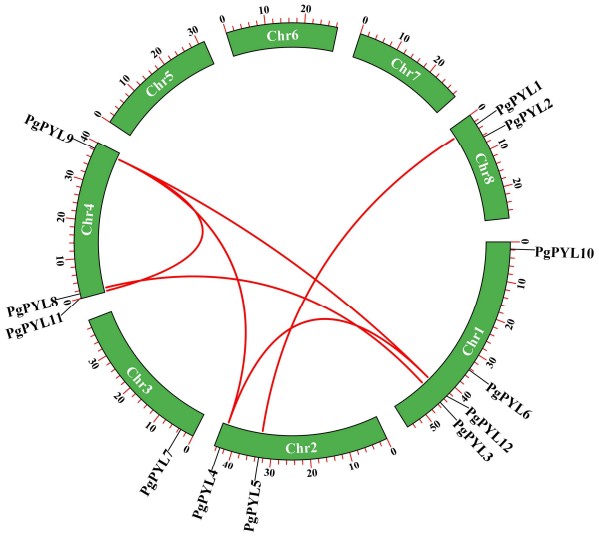


**Figure 6.** Collinearity analysis of the *PgPYL* genes. The red lines denote the *PgPYL*-duplicated gene pairs.

The collinearity among *Arabidopsis*, tomato, and pomegranate genes was analyzed (Figure 7) to ascertain the homology between the *PgPYL* genes and other plants. There were 21 pairs of collinearities observed in pomegranate and *Arabidopsis* and 28 pairs of collinearities in pomegranate and tomato. Several *PgPYL* genes were linked to at least two pairs of collinearities. In particular, *PgPYL1*, *PgPYL4*, *PgPYL5*, and *PgPYL9* were closely linked to the remainder of the genome and likely played significant components in the evolution of the *PYL* gene family. The collinearity analyses of the *PYLs* in pomegranate trees and other plants hold significant importance in establishing interspecific affinities and predicting gene functions.

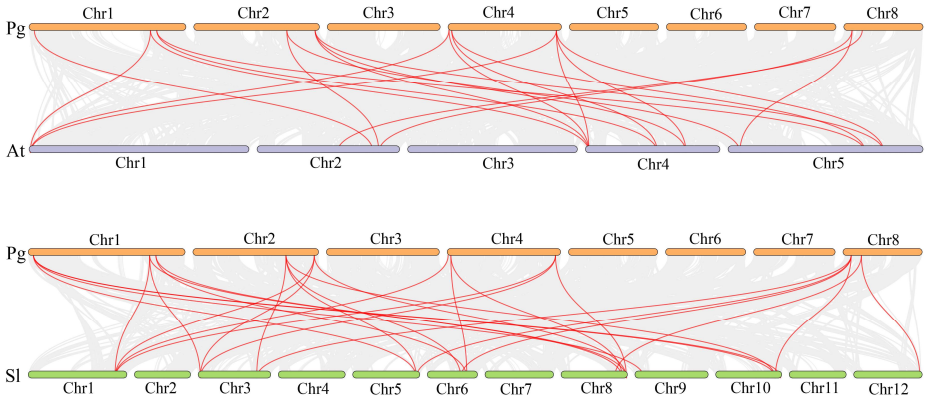


**Figure 7.** Syntenic relationships of the *PYL* gene family in pomegranate (*Punica granatum* L.) with Arabidopsis (*Arabidopsis thaliana* L.) and tomato (*Solanum lycopersicum* L.). Red lines denote the syntenic gene pairs of *PYLs*.

The Ka/Ks rate plays a crucial role in the evolutionary analysis of gene families and can be used to evaluate the existence of selective pressure on the gene encoding the protein. Ks denotes a synonymous substitution rate, which does not impact the type of amino acid, while Ka represents a nonsynonymous substitution rate, which modifies the expression of the amino acid. Nonsynonymous substitutions are predominantly detrimental, and purifying selection promotes their gradual decrease. A few nonsynonymous substitutions confer benefits to the organism, and base substitutions are retained by positive selection [52]. The Ka/Ks analysis between the coding regions of the *PgPYLs* (Table 1) revealed that the Ka/Ks is less than 1, suggesting that the *PgPYL* genes were subjected to purify selection.

**Table 1.** Selection pressure analysis of *PgPYL* gene family.

| Gene Pairs | Nonsynonymous Substitution Rate, Ka | Synonymous Substitution Rate, Ks | Ka/Ks |
|---|---|---|---|
| *PgPYL1* and *PgPYL5* | 0.2414 | 0.8796 | 0.2744 |
| *PgPYL3* and *PgPYL8* | 0.2350 | 0.8092 | 0.2904 |
| *PgPYL4* and *PgPYL9* | 0.1065 | 1.3583 | 0.0784 |
| *PgPYL4* and *PgPYL12* | 0.1860 | 1.9159 | 0.0971 |
| *PgPYL9* and *PgPYL11* | 0.1634 | 1.2598 | 0.1297 |

### *3.7. Expression of PgPYLs under ABA Treatment*

After 100 μmol/L ABA treatment, the relative expression levels of *PgPYLs* were detected using quantitative real-time PCR (qRT-PCR). The findings (Figure 8) indicate that the presence of the *PgPYL* genes exhibited diverse responses to ABA, accompanied by notable variations in relative expression levels. Eight genes (*PgPYL1*, *PgPYL2*, *PgPYL3*, *PgPYL4*, *PgPYL7*, *PgPYL8*, *PgPYL9*, and *PgPYL11*) exhibited up-regulation in expression. In comparison, four genes (*PgPYL5*, *PgPYL6*, *PgPYL10*, and *PgPYL12*) showed down-regulation. It was speculated that *PgPYL* genes had positive and negative responses to 100 μmol/L ABA treatment. Throughout the course of the treatment, the relative expression patterns of *PgPYL1*, *PgPYL2*, *PgPYL3*, *PgPYL7*, *PgPYL8*, and *PgPYL9* all displayed a similar tendency, with an initial rise, followed by a decline and then another increase. Notably, *PgPYL5* exhibited low expression or was hardly expressed from 2 h to 48 h. Besides *PgPYL5*, *PgPYL6*, *PgPYL10*, and *PgPYL12*, the relative expression of the remaining eight genes rose significantly after 2 h of ABA experiment. Subsequently, after 24 h of ABA treatment, the relative expression of the remaining nine genes demonstrated a decreasing trend, except for *PgPYL1*, *PgPYL3*, and *PgPYL6*.

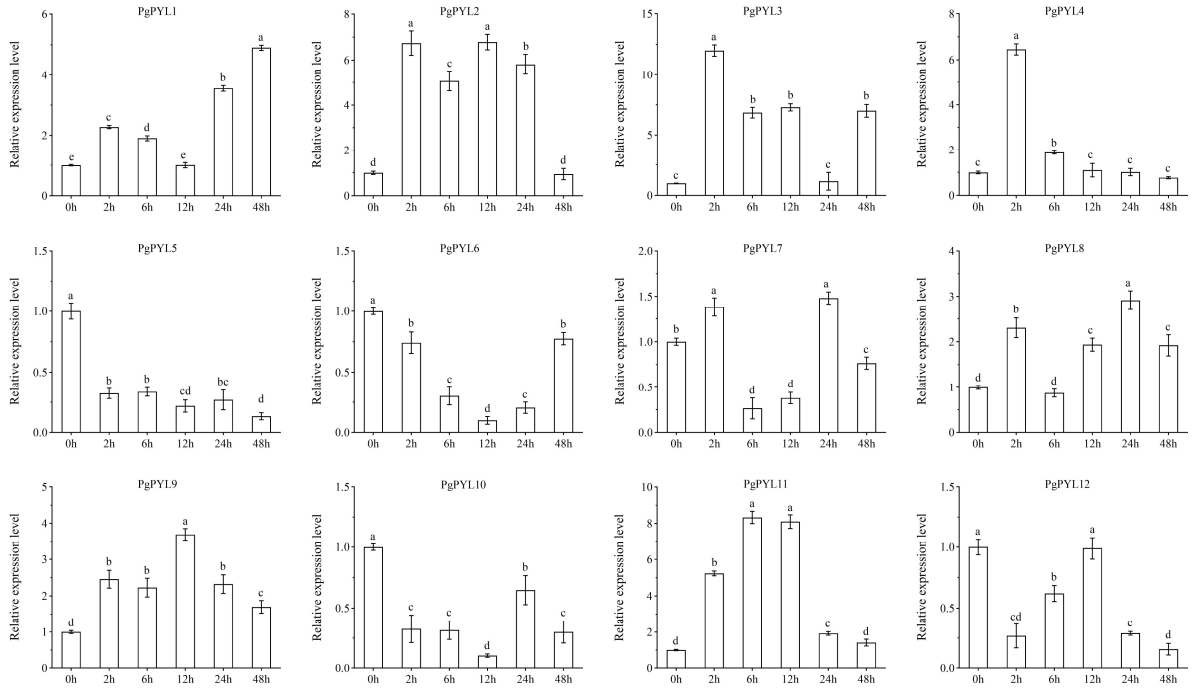


**Figure 8.** Expression patterns of the *PgPYL* gene family under 100 μmol/L ABA treatment. Pomegranate leaves were randomly collected at 0 (control check), 2, 6, 12, 24, and 48 h after treatment. Each gene's relative expression was calculated using the $2^{-\Delta\Delta Ct}$ method with *PgActin* serving as an internal control. The data show the mean ± SD of three biological replicates. The vertical bars show the standard error. Bars with different letters (a–e) indicate significant differences at $p < 0.05$ according to Duncan's test.

### *3.8. Gene Clone*

We extracted the total RNA from 'Tunisia' pomegranate leaves and reverse-transcribed it into cDNA. The PCR-amplificated product was identified by 1% agarose gel electrophoresis. The results (Figure 9A) show that there was a clear and bright band between 500 and 750 bp for *PgPYL1*, which was consistent with the predicted size of the amplified fragment. Subsequently, the target fragment was recovered, ligated, transformed, and sequenced. The sequencing outcomes (Figure 9B) demonstrated that the cloned *PgPYL1* was identical to the expected results, and the coding region of *PgPYL1* was obtained, with a length of 657 bp, encoding 218 amino acids. The gene contained the complete *PYR_PYL_RCAR_like* conserved structural domain.

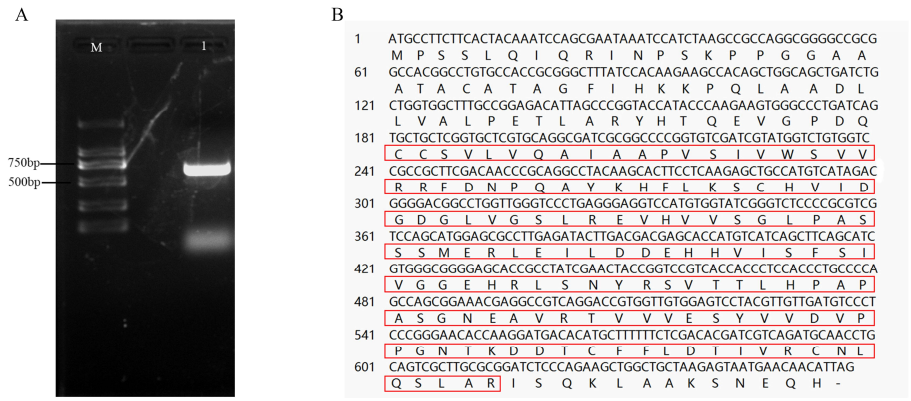


**Figure 9.** *PgPYL1* gene clone. (**A**) PCR amplification, M: DL ladder 2000 DNA Marker; 1: *PgPYL1*. (**B**) CDS sequence and coding amino acid sequence. The red square is the *PYR_PYL_RCAR_like* domain.

### *3.9. Tobacco Transient Expression Analysis*

The constructed pBI121-*PgPYL1* vector was subjected to transient expression analysis in tobacco, as shown in Figure 10B; in tobacco, the *PgPYL1* gene was significantly more highly expressed than both the wild-type (WT) and the unloaded pBI121. The data showed a tendency of rising and then falling over time, with a notable increase in the expression level starting on day 3 and reaching the highest level on day 5. The expression level was 6.64 times more than that of wild-type (WT) and 2.09 times higher than that of unloaded pBI121, and following the fifth day, the expression level began to decline. Furthermore, we measured the expression patterns of genes associated with the ABA signaling system in tobacco leaves. The data demonstrated that the *NtPP2C* genes' relative expression levels were down-regulated (Figure 10C), and the gene expression was substantially lower than that of the wild-type (WT) and the unloaded pBI121. In contrast, the *NtSnRK2* and *NtAREB* genes' expression levels were up-regulated and exhibited a tendency of increasing and then decreasing with the change in time, which was basically consistent with the tendency of *PgPYL1* gene expression in tobacco leaves (Figure 10D,E), suggesting that the overexpression of *PgPYL1* in tobacco may lead to a considerable up-regulation of *NtSnRK2* and *NtAREB* expression and a down-regulation of *NtPP2C* expression in tobacco leaves.

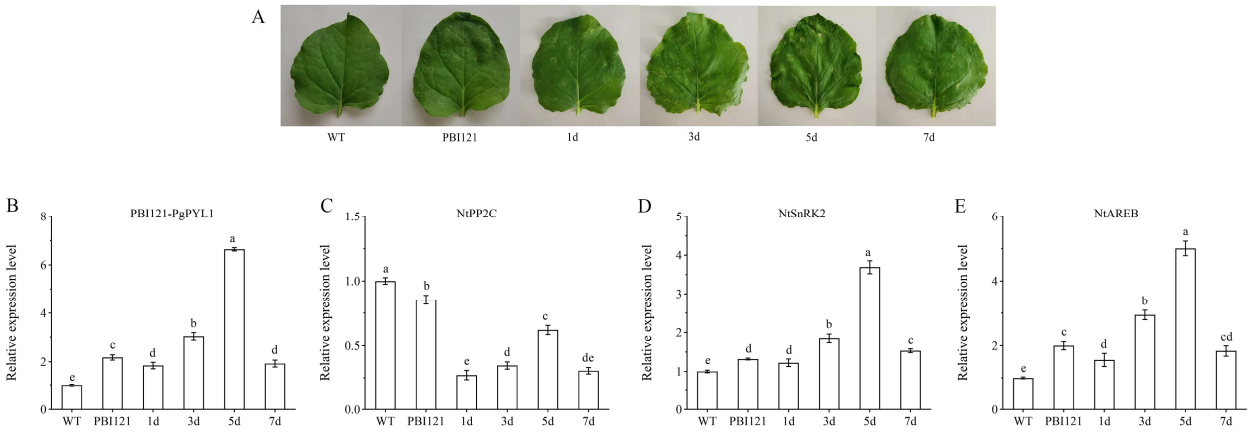


**Figure 10.** Tobacco transient expression. (**A**) Images of wild-type (WT), PBI121-overexpression, and *PgPYL1*-overexpression tobacco leaves. (**B**) *PgPYL1* expression, (**C**) *NtPP2C* expression, (**D**) *NtSnRK2* expression, and (**E**) *NtAREB* expression in WT, PBI121-overexpression, and *PgPYL1*-overexpression tobacco leaves. Bars with different letters (a–e) indicate significant differences at $p < 0.05$ according to Duncan's test.

## 4. Discussion

In orchestrating plant growth, development, and responses to both abiotic and biotic stresses, abscisic acid (ABA) assumes a pivotal role [53]. Positioned at the forefront of the ABA signaling regulation pathway, the *PYL* gene family stands out as an extensive group of phytohormone receptor genes primarily responsible for detecting ABA signals and initiating signaling [19]. Its significant contributions extend to influencing plant physiological and biochemical responses. Over recent years, the widespread presence of *PYL* genes has been unveiled in various species, such as tomato [26], grape [27], apple [54], and sweet cherry [55]. Environmental adversities, encompassing high salinity, drought, and low temperature, pose significant threats to normal plant growth, inhibiting photosynthesis, leading to premature plant failure, and ultimately affecting yield. The pomegranate industry, including fruit, seedlings, and processing, holds promising potential for development. However, their susceptibility to unfavorable environmental conditions jeopardizes pomegranates' yield and quality, resulting in considerable economic losses. Therefore, a crucial imperative emerges to excavate the function of the *PYL* gene family in pomegranates.

The discovery of 12 *PgPYL* genes through homology matching with known *PYL* protein sequences in *Arabidopsis* represents a noteworthy contribution. Notably, the variability in the number of *PgPYL* genes is comparatively lower than that observed in other species, such as *Arabidopsis* [19] (14), rice [23] (13), tomato [26] (14), and sweet cherry [55] (11). Chromosomal localization analysis unveiled a higher-density distribution of *PgPYL* genes on chromosomes 1 and 4 (Figure 1), hinting at potential tandem gene duplication. Physicochemical properties analysis characterized *PgPYL* proteins as acidic, with a negative total average hydrophilicity, rendering them hydrophilic. Secondary structure analysis indicated prevalent α-helices, extended strands, and random coils, which is consistent with studies on maize [56] and grape [57]. Subcellular localization analysis suggests a predominant expression of *PgPYL* genes in the cytoplasm, aligning with observations on *Arabidopsis* [19] and hazel [58]. Combining sequences from pomegranate, *Arabidopsis*, grape, tomato, and strawberry plants, an evolutionary tree built with the maximum likelihood method categorized the *PYL* gene family in pomegranate into three subgroups, aligning with classification outcomes of *Arabidopsis* [19] and maize [56].

Insights into the *PgPYL* protein sequences reveal binding sites for ABA, specifically within the conserved structural domains CL2 (gate) and CL4 (latch). This GATE-LATCH structure interacts with the ABA molecule, inducing conformational changes that form a surface interacting with *PP2C* proteins [59]. Mutations in certain structural domains suggest potential

associations with executive function. Conserved motif analysis identified 12 motifs within the *PgPYL* family, with subgroups exhibiting similar motif numbers and types, indicating close evolutionary relationships and probable functional similarities [60,61]. Examination of the exon–intron gene structure highlighted that four genes (*PgPYL1*, *PgPYL5*, *PgPYL6*, and *PgPYL7*) lack introns, signifying a high level of conservation and potential representation of a more primitive evolutionary state. The remaining members with 1–2 introns may have evolved from other family members through mechanisms like exon shuffling.

Analyses of promoter cis-acting elements are helpful for predicting the potential functions of genes. The promoter region of the *PgPYL* genes contains various cis-elements, mainly involving light-responsive elements, hormone-responsive elements, stress-responsive elements, and growth and development-related elements. So, we speculate that the *PgPYL* genes not only regulate growth, development, and stress tolerance, but also that their expression is influenced by hormones and the environment during growth. In pomegranates, *PgPYL* gene family members contain 33 cis-type elements, 13 elements of which are related to light response, accounting for a large proportion, suggesting that *PgPYL* genes are affected by light regulation during growth and development, which is consistent with the results of strawberry [25] and wild emmer wheat [62] studies. Transcription factor MYB binding sites were found in the promoter region, among which MBS mainly participates in drought induction [49]. Eight *PgPYL* genes contain 1–3 MBS elements, with *PgPYL1* having the most MBS elements, suggesting that this gene may be involved in regulating the drought-response mechanism. In addition, there are also some genes, such as *PgPYL9*, containing meristem-expression regulatory elements (CAT-box) and an element involved in zein metabolism regulation (O2-site); *PgPYL6* has a cell cycle regulation element (MSA-like) and involvement in the regulation of flavonoid biosynthesis (MBSI); and *PgPYL2* has an element controlling circadian rhythms (circadian), indicating that these *PgPYL* genes may be involved in regulating pomegranate development and secondary metabolism. Hormonal signals play an important role in plant resistance to drought and other stress conditions. Among the twelve members of the *PYL* gene family, nine *PgPYL* genes have ABRE elements, while a few genes do not have ABRE elements, a phenomenon also present in other species such as sweet cherry [55], soybean [63], and tea tree [64]. In addition, the promoter region of the *PgPYL* genes also contains response elements for various hormones such as auxin, gibberellin, jasmonic acid, and salicylic acid, further indicating that the *PgPYL* genes play an important role in stress tolerance and may be influenced by various hormones, involving a more complex multi-hormone signaling transduction network, consistent with the results of soybean research [65].

Gene duplication research within the *PgPYL* gene family had advanced our knowledge of the expansion and functionality of the specific gene family. The examination of the duplication of the *PgPYLs* reveals six pairs of colinear genes, suggesting that these colinear genes may have arisen from gene duplication. The process of gene duplication can lead to the creation of multiple duplicated genes in the genomes of plants. Furthermore, the existence of duplicate genes may facilitate the emergence of novel gene functions and improve plants' capacity for environmental adaptation [66]. Moreover, to enhance further knowledge of the evolutionary relationship of the *PYL* gene family in pomegranates, 21 and 28 homologous chromosome pairs have been identified in pomegranate, *Arabidopsis*, and tomato plants. Purifying selection in *PgPYL* genes implies their crucial role in plant adaptation to adverse conditions. However, in the phylogenetic analysis, some of these genes seemed to have no evolutionary origin consistent with gene duplication, such as *PgPYL9* and *PgPYL11*. We speculate that gene rearrangement events within the gene family may have occurred, leading to changes in the gene sequence. This change may affect the outcome of gene replication, or the evolutionary origin of some genes seems inconsistent with the gene duplication results due to the use of different algorithms and models to construct phylogenetic trees.

In this study, pomegranate leaves were treated with 100 μmol/L ABA. The qRT-PCR data showed that most *PgPYL* genes were significantly up-regulated, and it was

speculated that the *PgPYL* genes may be involved in endogenous ABA signaling and plant response to exogenous ABA. The outcome was consistent with previous research on tomatoes [67]. In other plants, for example, applying 100 μmol/L ABA to pears found that the expression levels of the remaining nine *PbrPYL* genes except *PbrPYL4* and *PbrPYL6* were up-regulated [61]. Applying 200 μmol/L ABA to sweet cherries found that the expression levels of *PaPYL6*, *PaPYL7*, *PaPYL8* and *PaPYL10* genes were up-regulated [55]. It seems that the expression patterns of *PYL* genes are diverse in different species. It is worth noting that we found that *PgPYL6* has 16 ABRE elements, but the expression level showed a downward trend. We speculated whether the gene is sensitive to high-concentration ABA treatment, thereby inhibiting its expression level. In addition, we found that the *PgPYL6* gene's expression level began to increase after 48 h of ABA treatment. It is speculated that this gene may also be involved in its adaptive regulation in the later stages of hormone stress. This requires further verification in our future experiments. This phenomenon is also seen in sweet cherry [55], where *PaPYL5* has five AREB elements, but after applying 200 μmol/L ABA, the expression level of the gene is down-regulated; *PaPYL6* and *PaPYL10* do not have ABRE elements, but at 12 h after treatment, the expression level is significantly higher than 0 h, so we guess there appears to be no correlation between gene expression levels and the ABA response elements found. Combined with the phylogenetic tree, it was found that *PgPYL4*, *PgPYL9*, and *PgPYL11* whose expression levels increased after ABA treatment were located in Group I; *PgPYL2*, *PgPYL3*, *PgPYL7*, and *PgPYL8* were located in Group II; while *PgPYL5*, *PgPYL6*, and *PgPYL10* whose expression levels decreased were located in Group III, so it is speculated that there may be a certain correlation between the evolutionary tree classification results and the expression levels of genes. This finding is consistent with the research on pears [61] and sweet cherries [55].

Studies have found that overexpression of *AtPYL4*, *AtPYL5* and *AtPYL9* genes in *Arabidopsis* can not only significantly increase the sensitivity of plants to ABA in stages such as seed germination, seedling growth, and stomatal opening and closing, but also improve the plant's drought resistance [20,21]. In addition, some scholars have found that the overexpression of ABA receptors can enhance the sensitivity of transgenic plants to ABA and improve the tolerance of these plants to abiotic stress. For example, in maize, *ZmPYL8*, *ZmPYL9,* and *ZmPYL12* play an important role in plant drought tolerance [28]. In rice, *OsPYL/RCAR5* has been reported to positively regulate ABA signaling, including increasing the sensitivity of seeds to ABA during germination and seedling growth stages and improving rice's resistance to drought and salt-alkali stress [30,31]. In wheat, overexpression of *TaPYL4* increased the sensitivity of wheat to ABA, reduced stomatal pore size and transpiration, and improved wheat yield and WUE (Water Usage Effectiveness) under drought conditions [68]. In this study, *PgPYL1* was transiently expressed in tobacco, and qPCR technology was used to detect genes related to the ABA signaling pathway in tobacco. In the ABA signaling pathway, *SnRK2* is a positive regulator, *PP2C* is a negative regulator, and *AREB* is the core transcription factor of the ABA signaling pathway and participates in signal transduction. The data showed that the expression of *NtPP2C* was generally down-regulated, while the expression of *NtSnRK2* and *NtAREB* was generally up-regulated. The expression of *PgPYL1* was consistent with the expression of the *NtSnRK2* and *NtAREB* genes, showing a trend of first increasing and then decreasing (Figure 10). It is speculated that *PgPYL1* may be involved in the ABA signal transduction pathway; however, the specific functional information of *PgPYL1* needs to be further explored and verified in future experiments.

## 5. Conclusions

In this investigation, our scrutiny of the pomegranate 'Tunisia' genome led to the identification of 12 *PgPYL* genes, each uniquely positioned on five distinct chromosomes. Employing phylogenetic research, we successfully classified the *PgPYL* gene family into three discernible subgroups. The comprehensive analysis of conserved motifs and intron–exon structures within this gene family unearthed noteworthy structural similarities among

genes within the same subgroup, suggesting potential functional congruence in their encoded proteins. A pivotal observation emerged from our exploration of the amplification mechanisms within the *PgPYL* gene family, emphasizing fragment duplication as the primary mechanism. This mechanism not only shed light on the evolutionary dynamics of the gene family but also underscored the significance of this process in shaping the genomics of pomegranates. Delving into the regulatory elements governing *PgPYL* gene expression, our investigation of cis-acting elements within the promoter region unveiled the genes' responsiveness to a spectrum of stimuli, encompassing hormonal cues and abiotic stressors. This finding adds a layer of complexity to our understanding of how *PgPYL* genes integrate various signals, contributing to the plant's adaptive responses. The culmination of our efforts in this study resides in the qRT-PCR data, which provide compelling evidence implicating *PgPYL* genes in the plant's response to exogenous ABA. This insight into their involvement in ABA signaling pathways positions *PgPYL* genes as key players in the intricate molecular machinery orchestrating the plant's reactions to environmental stimuli. The results of tobacco transient expression demonstrated that the expression of pBI121-*PgPYL1* and the related genes of the ABA signaling pathway showed a consistent tendency of rising and then decreasing.

In conclusion, our investigation serves as a foundational exploration into the *PgPYL* gene family function, unraveling key aspects of their genomic organization, evolutionary history, and responsiveness to crucial signaling pathways. This study not only expands our knowledge of pomegranate genetics but also presents a reservoir of potential candidate genes for future endeavors in genetic engineering and pomegranate breeding. As we delve deeper into the intricate network of plant molecular responses, this work paves the way for additional inquiries, promising a more nuanced understanding of the *PgPYL* gene family's role in shaping the adaptive strategies of pomegranate in dynamic environments.

**Supplementary Materials:** The following supporting information can be downloaded at: https://www.mdpi.com/article/10.3390/horticulturae10050502/s1, Table S1: Primer sequences; Table S2: Physicochemical properties, secondary structure and subcellular localization of PgPYL proteins; Table S3: Information of constructing phylogenetic tree; Table S4: The cis-acting elements of PgPYLs.

**Author Contributions:** Conceptualization, K.Y. and Z.Y.; methodology, K.Y.; software, K.Y. and F.C.; validation, K.Y., F.C. and H.R.; formal analysis, K.Y. and J.H.; data curation, K.Y.; writing—original draft preparation, K.Y.; writing—review and editing, H.R., X.Z. and Z.Y.; visualization, K.Y.; supervision, Z.Y.; funding acquisition, Z.Y. All authors have read and agreed to the published version of the manuscript.

**Funding:** This research received no external funding.

**Data Availability Statement:** The raw data supporting the conclusions of this article will be made available by the authors on request.

**Conflicts of Interest:** The authors declare no conflicts of interest.

## References

1. Yuan, Z.; Fang, Y.; Zhang, T.; Fei, Z.; Han, F.; Liu, C.; Liu, M.; Xiao, W.; Zhang, W.; Wu, S.; et al. The pomegranate (*Punica granatum* L.) genome provides insights into fruit quality and ovule developmental biology. *Plant Biotechnol. J.* **2018**, *16*, 1363–1374. [CrossRef]
2. Ben, L.; Kim, K.; Quah, C.; Kim, W.; Shahimi, M. Anti-inflammatory potential of ellagic acid, gallic acid and punicalagin A&B isolated from Punica granatum. *BMC Complement. Altern. Med.* **2017**, *17*, 47–57. [CrossRef] [PubMed]
3. Qin, G.; Xu, C.; Ming, R.; Tang, H.; Guyot, R.; Kramer, E.M.; Hu, Y.; Yi, X.; Qi, Y.; Xu, X.; et al. The pomegranate (*Punica granatum* L.) geneme and the genomics of punicalagin biosynthesis. *Plant J.* **2017**, *91*, 1108–1128. [CrossRef] [PubMed]
4. Chen, L.; Zhang, J.; Li, H.; Niu, J.; Xue, H.; Liu, B.; Wang, Q.; Luo, X.; Zhang, F.; Zhao, D.; et al. Transcriptomic Analysis Reveals Candidate Genes for Female Sterility in Pomegranate Flowers. *Front. Plant Sci.* **2017**, *8*, 1430. [CrossRef] [PubMed]
5. Finkelstein, R.R.; Gampala, S.S.; Rock, C.D. Abscisic acid signaling in seeds and seedlings. *Plant Cell* **2002**, *14*, S15–S45. [CrossRef] [PubMed]

6. Sreenivasulu, N.; Radchuk, V.; Strickert, M.; Miersch, O.; Weschke, W.; Wobus, U. Gene expression patterns reveal tissue-specific signaling networks controlling programmed cell death and ABA-regulated maturation in developing barley seeds. *Plant J.* **2006**, *47*, 310–327. [CrossRef] [PubMed]
7. Zhu, J.K. Salt and drought stress signal transduction in plants. *Annu. Rev. Plant Biol.* **2002**, *53*, 247–273. [CrossRef]
8. Melcher, K.; Ng, L.M.; Zhou, X.E.; Soon, F.F.; Xu, Y.; Park, S.Y.; Weiner, J.J.; Fujii, H.; Chinnusamy, V.; Kovach, A.; et al. A gate-latch-lock mechanism for hormone signalling by abscisic acid receptors. *Nature* **2009**, *462*, 602–608. [CrossRef] [PubMed]
9. Santiago, J.; Rodrigues, A.; Saez, A.; Rubio, S.; Antoni, R.; Dupeux, F.; Park, S.Y.; Márquez, J.A.; Cutler, S.R.; Rodriguez, P.L. Modulation of drought resistance by the abscisic acid receptor PYL5 through inhibition of clade A PP2Cs. *Plant J.* **2009**, *60*, 575–588. [CrossRef]
10. Umezawa, T.; Sugiyama, N.; Mizoguchi, M.; Hayashi, S.; Myouga, F.; Yamaguchi, S.K.; Ishihama, Y.; Hirayama, T.; Shinozaki, K. Type 2C protein phosphatases directly regulate abscisic acid-activated protein kinases in Arabidopsis. *Proc. Natl. Acad. Sci. USA* **2009**, *106*, 17588–17593.
11. Schweighofer, A.; Hirt, H.; Meskiene, I. Plant PP2c phosphatases: Emerging functions in stress signaling. *Trends Plant Sci.* **2004**, *9*, 236–243. [CrossRef] [PubMed]
12. Saavedra, X.; Modrego, A.; Rodríguez, D.; GonzálezG, M.P.; Sanz, L.; Nicolás, G.; Lorenzo, O. The nuclear interactor PYL8/RCAR3 of Fagus sylvatica FsPP2C1 is a positive regulator of abscisic acid signaling in seeds and stress. *Plant Physiol.* **2010**, *152*, 133–150. [CrossRef] [PubMed]
13. Yuan, X.; Yin, P.; Hao, Q.; Yan, C.; Wang, J.; Yan, N. Single amino acid alteration between valine and isoleucine determines the distinct pyrabactin selectivity by PYL1 and PYL2. *J. Biol. Chem.* **2010**, *285*, 28953–28958. [CrossRef] [PubMed]
14. Fujita, Y.; Nakashima, K.; Yoshida, T.; Katagiri, T.; Kidokoro, S.; Kanamori, N.; Umezawa, T.; Fujita, M.; Maruyama, K.; Ishiyama, K.; et al. Three SnRK2 protein kinases are the main positive regulators of abscisic acid signaling in response to water stress in Arabidopsis. *Plant Cell Physiol.* **2009**, *50*, 2123–2132. [CrossRef] [PubMed]
15. Sirichandra, C.; Davanture, M.; Turk, B.E.; Zivy, M.; Valot, B.; Leung, J.; Merlot, S. The arabidopsis ABA-activated kinase OST1 phosphorylates the bZIP transcription factor ABF3 and creates a 14-3-3 binding site involved in its turnover. *PLoS ONE* **2010**, *5*, e13935. [CrossRef] [PubMed]
16. Hubbard, K.E.; Nishimura, N.; Hitomi, K.; Getzoff, E.D.; Schroeder, J.I. Early abscisic acid signal transduction mechanisms: Newly discovered components and newly emerging questions. *Genes Dev.* **2010**, *24*, 1695–1708. [CrossRef] [PubMed]
17. Yoshida, T.; Fujita, Y.; Sayama, H.; Kidokoro, S.; Maruyama, K.; Mizoi, J.; Shinozaki, K.; YamaguchiS, K. AREB1, AREB2, and ABF3 are master transcription factors that cooperatively regulate ABRE-dependent ABA signaling involved in drought stress tolerance and require ABA for full activation. *Plant J.* **2010**, *61*, 672–685. [CrossRef] [PubMed]
18. Ma, Y.; Szostkiewicz, I.; Korte, A.; Moes, D.; Yang, Y.; Christmann, A.; Grill, E. Regulators of PP2C phosphatase activity function as abscisic acid sensors. *Science* **2009**, *324*, 1064–1068. [CrossRef]
19. Park, S.Y.; Fung, P.; Nishimura, N.; Jensen, D.R.; Fujii, H.; Zhao, Y.; Lumba, S.; Santiago, J.; Rodrigues, A.; Chow, T.F.; et al. Abscisic acid inhibits type 2C protein phosphatases via the PYR/PYL family of START proteins. *Science* **2009**, *324*, 1068–1071. [CrossRef]
20. Santiago, J.; Dupeux, F.; Round, A.; Antoni, R.; Park, S.Y.; Jamin, M.; Cutler, S.R.; Rodriguez, P.L.; Márquez, J.A. The abscisic acid receptor PYR1 in complex with abscisic acid. *Nature* **2009**, *462*, 665–683. [CrossRef]
21. Shi, H.; Ye, T.; Zhu, J.K.; Chan, Z. Constitutive production of nitric oxide leads to enhanced drought stress resistance and extensive transcriptional reprogramming in Arabidopsis. *J. Exp. Bot.* **2014**, *65*, 4119–4931. [CrossRef] [PubMed]
22. Bai, G.; Xie, H.; Yao, H.; Li, F.; Chen, X.; Zhang, Y.; Xiao, B.; Yang, J.; Li, Y.; Yang, D.H. Genome-wide identification and characterization of ABA receptor PYL/RCAR gene family reveals evolution and roles in drought stress in Nicotiana tabacum. *BMC Genom.* **2019**, *20*, 575. [CrossRef] [PubMed]
23. He, Y.; Hao, Q.; Li, W.; Yan, C.; Yan, N.; Yin, P. Identification and characterization of ABA receptors in Oryza sativa. *PLoS ONE* **2014**, *9*, e95246. [CrossRef]
24. Wang, Y.; Fu, F.; Yu, H.; Hu, T.; Zhang, Y.; Tao, Y.; Zhu, J.; Zhao, Y.; Li, W. Interaction network of core ABA signaling components in maize. *Plant Mol. Biol.* **2018**, *96*, 245–263. [CrossRef]
25. Chai, Y.M.; Jia, H.F.; Li, C.L.; Dong, Q.H.; Shen, Y.Y. FaPYR1 is involved in strawberry fruit ripening. *J. Exp. Bot.* **2011**, *62*, 5079–5089. [CrossRef] [PubMed]
26. Sun, L.; Wang, Y.P.; Chen, P.; Ren, J.; Ji, K.; Li, Q.; Li, P.; Dai, S.J.; Leng, P. Transcriptional regulation of SlPYL, SlPP2C, and SlSnRK2 gene families encoding ABA signal core components during tomato fruit development and drought stress. *J. Exp. Bot.* **2011**, *62*, 5659–5669. [CrossRef] [PubMed]
27. Boneh, U.; Biton, I.; Zheng, C.; Schwartz, A.; Ben-Ari, G. Characterization of potential ABA receptors in Vitis vinifera. *Plant Cell Rep.* **2012**, *31*, 311–321. [CrossRef]
28. He, Z.; Zhong, J.; Sun, X.; Wang, B.; Terzaghi, W.; Dai, M. The maize ABA receptors ZmPYL8, 9, and 12 facilitate plant drought resistance. *Front. Plant Sci.* **2018**, *9*, 422. [CrossRef]
29. Yu, J.; Ge, H.; Wang, X.; Tang, R.; Wang, Y.; Zhao, F.; Lan, W.; Luan, S.; Yang, L. Overexpression of pyrabactin resistance-like abscisic acid receptors enhances drought, osmotic, and cold tolerance in transgenic poplars. *Front. Plant Sci.* **2017**, *8*, 1752. [CrossRef]

30. Kim, H.; Hwang, H.; Hong, J.W.; Lee, Y.N.; Ahn, I.P.; Yoon, I.S.; Yoo, S.D.; Lee, S.; Lee, S.C.; Kim, B.G. A rice orthologue of the ABA receptor, OsPYL/RCAR5, is a positive regulator of the ABA signal transduction pathway in seed germination and early seedling growth. *J. Exp. Bot.* **2012**, *63*, 1013–1024. [CrossRef]
31. Kim, H.; Lee, K.; Hwang, H.; Bhatnagar, N.; Kim, D.Y.; Yoon, I.S.; Byun, M.O.; Kim, S.T.; Jung, K.H.; Kim, B.G. Overexpression of PYL5 in rice enhances drought tolerance, inhibits growth, and modulates gene expression. *J. Exp. Bot.* **2014**, *65*, 453–464. [CrossRef] [PubMed]
32. Altschul, S.F.; Gish, W.; Miller, W.; Myers, E.W.; Lipman, D.J. Basic local alignment search tool. *J. Mol. Biol.* **1990**, *215*, 403–410. [CrossRef] [PubMed]
33. Finn, R.D.; Clements, J.; Eddy, S.R. HMMER web server: Interactive sequence similarity searching. *Nucleic Acids Res.* **2011**, *39*, W29–W37. [CrossRef] [PubMed]
34. Chao, J.; Li, Z.; Sun, Y.; Aluko, O.O.; Wu, X.; Wang, Q.; Liu, G. MG2C: A user-friendly online tool for drawing genetic maps. *Mol. Hortic.* **2021**, *1*, 16. [CrossRef] [PubMed]
35. Artimo, P.; Jonnalagedda, M.; Arnold, K.; Baratin, D.; Csardi, G.; Duvaud, S.; Flegel, V.; Fortier, A.; Gasteiger, E.; Grosdidier, A. ExPASy: SIB bioinformatics resource portal. *Nucleic Acids Res.* **2012**, *40*, W597–W603. [CrossRef] [PubMed]
36. Petersen, T.N.; Brunak, S.; Heijne, G.; Nielsen, H. SignalP 4.0: Discriminating signal peptides from transmembrane regions. *Nat. Methods* **2011**, *8*, 785–786. [CrossRef] [PubMed]
37. Geourjon, C.; Deléage, G. SOPMA: Significant improvements in protein secondary structure prediction by consensus prediction from multiple alignments. *Comput. Appl. Biosci.* **1995**, *11*, 681–684. [CrossRef] [PubMed]
38. Chou, K.C.; Shen, H.B. Plant-mPLoc: A top-down strategy to augment the power for predicting plant protein subcellular localization. *PLoS ONE* **2010**, *5*, e11335. [CrossRef] [PubMed]
39. Tamura, K.; Stecher, G.; Kumar, S. MEGA11: Molecular Evolutionary Genetics Analysis Version 11. *Mol. Biol. Evol.* **2021**, *38*, 3022–3027. [CrossRef]
40. Bailey, T.L.; Boden, M.; Buske, F.A.; Frith, M.; Grant, C.E.; Clementi, L.; Ren, J.; Li, W.W.; Noble, W.S. MEME SUITE: Tools for motif discovery and searching. *Nucleic Acids Res.* **2009**, *37*, 202–208. [CrossRef]
41. Hu, B.; Jin, J.; Guo, A.Y.; Zhang, H.; Luo, J.; Gao, G. GSDS 2.0: An upgraded gene feature visualization server. *Bioinformatics* **2015**, *31*, 1296–1297. [CrossRef] [PubMed]
42. Chen, C.; Chen, H.; Zhang, Y.; Thomas, H.R.; Frank, M.H.; He, Y.; Xia, R. TBtools: An Integrative Toolkit Developed for Interactive Analyses of Big Biological Data. *Mol. Plant* **2020**, *13*, 1194–1202. [CrossRef] [PubMed]
43. Rombauts, S.; Déhais, P.; Montagu, M.V.; Rouzé, P. PlantCARE, a plant cis-acting regulatory element database. *Nucleic Acids Res.* **1999**, *27*, 295–296. [CrossRef] [PubMed]
44. Wang, Y.; Tang, H.; Debarry, J.D.; Tan, X.; Li, J.; Wang, X.; Lee, T.H.; Jin, H.; Marler, B.; Guo, H.; et al. MCScanX: A toolkit for detection and evolutionary analysis of gene synteny and collinearity. *Nucleic Acids Res.* **2012**, *40*, e49. [CrossRef] [PubMed]
45. Librado, P.; Rozas, J. DnaSP v5: A software for comprehensive analysis of DNA polymorphism data. *Bioinformatics* **2009**, *25*, 1451–1452. [CrossRef]
46. Livak, K.; Schmittgen, T. Analysis of relative gene expression data using real-time quantitative PCR and the $2^{-\Delta\Delta Ct}$ method. *Methods* **2001**, *25*, 402–408. [CrossRef] [PubMed]
47. Kai, W.; Wang, J.; Liang, B.; Fu, Y.; Zheng, Y.; Zhang, W.; Li, Q.; Leng, P. PYL9 is involved in the regulation of ABA signaling during tomato fruit ripening. *J. Exp. Bot.* **2019**, *70*, 6305–6319. [CrossRef] [PubMed]
48. Dalal, M.; Inupakutika, M. Transcriptional regulation of ABA core signaling component genes in sorghum (*Sorghum bicolor* L. Moench). *Mol. Breed.* **2014**, *34*, 1517–1525. [CrossRef]
49. Liu, J.H.; Peng, T.; Dai, W. Critical cis-acting elements and interacting transcription factors: Key players associated with abiotic stress responses in plants. *Plant Mol. Biol. Rep.* **2014**, *32*, 303–317. [CrossRef]
50. Cui, G.; Hou, J.; Tong, L.; Xu, Z. Light responsive elements and binding proteins of plant genes. *Plant Physiol. J.* **2010**, *46*, 991–1000.
51. Flagel, L.E.; Wendel, J.F. Gene duplication and evolutionary novelty in plants. *New Phytol.* **2009**, *183*, 557–564. [CrossRef] [PubMed]
52. Xia, Y.; Yan, Y. Advances in positive selection sites and their computational software. *J. Yangtze Univ. (Nat. Sci. Ed.)* **2016**, *13*, 51–53. [CrossRef]
53. Lee, S.C.; Luan, S. ABA signal transduction at the crossroad of biotic and abiotic stress responses. *Plant Cell Environ.* **2012**, *35*, 53–60. [CrossRef]
54. Hou, H.; Lv, L.; Huo, H.; Dai, H.; Zhang, Y. Genome-wide identification of the ABA receptors genes and their response to abiotic stress in apple. *Plants* **2020**, *9*, 1028. [CrossRef]
55. Zhou, J.; An, F.; Sun, Y.; Guo, R.; Pan, L.; Wan, T.; Hao, Y.; Cai, Y. Genome-wide identification of the ABA receptor *PYL* gene family and expression analysis in *Prunus avium* L. *Sci. Hortic.* **2023**, *313*, 111919. [CrossRef]
56. Li, H.; Wang, Y.; Zhang, X.; Fu, F.; Li, W. Bioinformatic analysis for abscisic acid perceptor gene family in maize. *J. Nucl. Agric. Sci.* **2015**, *29*, 1657–1667. [CrossRef]
57. Ma, Z.; Chen, B.; Li, W.; Mao, J. Identification and expression analysis of *PYL* gene families in grape. *J. Fruit Sci.* **2018**, *35*, 265–274. [CrossRef]
58. Zhang, X.; Zhao, Y.; Chen, Y.; Sun, B.; Liu, J. Genome-wide identification and expression analysis of *PYL* gene family in Corylus heterophylla during fruit development. *Acta Agric. Univ. Jiangxiensis* **2021**, *43*, 435–444. [CrossRef]

59. Yin, P.; Fan, H.; Hao, Q.; Yuan, X.; Wu, D.; Pang, Y.; Yan, C.; Li, W.; Wang, J.; Yan, N. Structural insights into the mechanism of abscisic acid signaling by PYL proteins. *Nat. Struct. Mol. Biol.* **2009**, *16*, 1230–1236. [CrossRef]
60. Zhang, Z.; Luo, S.; Liu, Z.; Wan, Z.; Gao, X.; Qiao, Y.; Yu, J.; Zhang, G. Genome-wide identification and expression analysis of the cucumber *PYL* gene family. *PeerJ* **2022**, *10*, 12786. [CrossRef]
61. Wang, G.; Qi, K.; Gao, X.; Guo, L.; Cao, P.; Li, Q.; Qiao, X.; Gu, C.; Zhang, S. Genome-wide identification and comparative analysis of the *PYL* gene family in eight Rosaceae species and expression analysis of seeds germination in pear. *BMC Genom.* **2022**, *23*, 233. [CrossRef]
62. Wang, Z.Y.; Yang, G.; Sai, N.; Pan, W.Q.; Song, W.N.; Nie, X.J. ldentification and expression analysis of *PYL* gene family in wild emmer wheat (*Triticum dicoccoides* L.) under abiotic stress. *J. Triticeae Crops* **2022**, *42*, 1–10.
63. Zhang, Z.; Ali, S.; Zhang, T.; Wang, W.; Xie, L. Identification, evolutionary and expression analysis of PYL-PP2C-SnRK2s gene families in soybean. *Plants* **2020**, *9*, 1356. [CrossRef] [PubMed]
64. An, Y.; Mi, X.; Xia, X.; Qiao, D.; Yu, S.; Zheng, H.; Jing, T.; Zhang, F. Genome-wide identification of the *PYL* gene family of tea plants (*Camellia sinensis*) revealed its expression profiles under different stress and tissues. *BMC Genom.* **2023**, *24*, 362. [CrossRef] [PubMed]
65. Zhang, Z.H.; Zhang, T.X.; Wang, W.P.; Xie, L.N. ldentification, phylogenetic evolution and expression analysis of abscisic acid receptors gene family in *Glycine max* L. Merr. *J. South. Agric.* **2020**, *51*, 1904–1916.
66. Panchy, N.; Lehti-Shiu, M.; Shiu, S. Evolution of gene duplication in plants. *Plant Physiol.* **2016**, *171*, 2294–2316. [CrossRef]
67. Wang, A.X.; Meng, L.J.; Chen, X.L.; Mo, F.L.; Lv, R.; Xue, X.P.; Meng, F.Y.; Qi, H.N.; Zhang, Z.Z. Genome-wide identification and expression analysis of abscisic acid receptor *PYL* gene family in tomato. *J. Northeast Agric. Univ.* **2023**, *54*, 21–32. [CrossRef]
68. Mega, R.; Abe, F.; Kim, J.S.; Tsuboi, Y.; Tanaka, K.; Kobayashi, H.; Sakata, Y.; Hanada, K.; Tsujimoto, H.; Kikuchi, J.; et al. Tuning water-use efficiency and drought tolerance in wheat using abscisic acid receptors. *Nat. Plants* **2019**, *5*, 153–159. [CrossRef]